Journal of Japan Association for Earthquake Engineering, Vol. 25, No. 8, 2025

PROPOSAL OF QUANTITATIVE EVALUATION METHOD FOR REDUNDANCY IN RAILWAY BRIDGES AND VIADUCTS

Kazunori WADA[1], Kimitoshi SAKAI[2] and Yoshikazu TAKAHASHI[3]

[1] Member, M. Eng., Senior Researcher, Railway Technical Research Institute, Tokyo, Japan, wada.kazunori.73@rtri.or.jp
[2] Member, Dr. Eng., Laboratory Head, Railway Technical Research Institute, Tokyo, Japan, sakai.kimitoshi.36@rtri.or.jp
[3] Member, Dr. Eng., Professor, Kyoto University, Kyoto, Japan, takahashi.yoshikazu.4v@kyoto-u.ac.jp

ABSTRACT: In recent years, a quantitative evaluation method for anti-catastrophe has been proposed. However, this is still conceptual, and it cannot be said that an evaluation method based on design practices has been established. Therefore, we focus on redundancy, which is one of the performance items of anti-catastrophe, and propose a quantitative evaluation method of redundancy for railway bridges and viaducts. In this method, the structural redundancy is evaluated from both perspectives, "margin" that means the displacement leading to collapse against the design limit displacement and "parallelism" that means the change in the margin when the column member disappears. And the structural analysis confirmed the validity of the method. By using this method, it becomes possible to explicitly consider redundancy in seismic design, diagnosis, reinforcement, etc.

Keywords: *Anti-catastrophe, Redundancy, Railway bridges and viaducts, Quantitative evaluation method*

1. INTRODUCTION

The 1995 South Hyogo Prefecture Earthquake and other similar events have promoted major developments in seismic design and reinforcement technology for transportation infrastructure such as railways and roads. However, unexpected earthquakes occur frequently, such as the 2011 Tohoku Earthquake that occurred in the Pacific Ocean reaching a magnitude of 9.0, and the 2016 Kumamoto Earthquake, which involved two earthquakes with a seismic intensity of 7. This led to a strong awareness regarding the challenges associated with such events that exceeded the existing seismic design. In response to these challenges, the "Design Standards for Railway Structures and Commentary (Seismic Design)"[1)] (hereinafter, "Seismic Standards") introduced the "anti-catastrophe" concept, which refers to the "prevention of structures or systems from reaching a catastrophe in response to an unexpected event," as a response capability against events that cannot be covered by the seismic design. This has been used as the basis for actively discussing the anti-catastrophe concept in various areas such as roads, railways, ports, and nuclear power[2)–7)], and to conduct structural examinations that actively implement anti-

catastrophe improvements[8), 9)].

Meanwhile, a method for evaluating the anti-catastrophe concept was not established when the Seismic Standards[1)] were revised, and has remained only a consideration in seismic structural planning. To address this lack of consideration, a method for evaluating the anti-catastrophe concept in railway structures with a focus on performance such as redundancy and robustness has been proposed in recent years[10)]. In addition, proposals have been presented for a design procedure that considers the anti-catastrophe concept in the waterworks field[11)]. Although these proposals remain conceptual, various elemental technologies need to be improved for their practical application. One example of an evaluation method for practical application is the anti-catastrophe structural planning method used for continuous truss bridges[12)]; however, methods for evaluating general railway bridges and viaducts are yet to be established.

Given these aspects, we focus on redundancy, which is considered to be a factor influencing the anti-catastrophe performance of railway structures[10)], and we propose a quantitative evaluation method. In Section 2, we summarize the concepts of redundancy examined in previous research and describe the concepts of redundancy and indicators for quantitative evaluation employed in this study. In Section 3, we present a practical evaluation method for the indices used to quantitatively assess the proposed redundancy with an assumption of application to design practice. In Section 4, we confirm the validity of the evaluation method proposed in Section 3 by comparing it with a detailed analysis using a 3D frame model. In Section 5, we estimate the redundancy using the proposed method for a general railway rigid-frame viaduct.

2. REDUNDANCY CONCEPTUALIZATION AND QUANTITATIVE EVALUATION METHOD

Redundancy has been considered and examined in a wide variety of fields, including civil engineering, architecture, machinery, and information. In this section, we summarize the concepts raised in previous research and discuss the concepts of redundancy and indices for the quantitative evaluation in this paper.

2.1 Summary of previous research

Redundancy commonly implies “extra” or “duplicate”; however, in the civil engineering and architecture fields, it is considered to have two perspectives: “margin,” which relates to a limit state, and “parallelism,” which focuses on the connections of members[13)].

The margin has been evaluated less from the perspective of redundancy and more in terms of the evaluation of the ultimate state of the member[14)] and seismic margin[15)]. The current seismic design of railway structures[1)] sets the state in which one member reaches its ultimate state as the safety limit; however, this is not necessarily the ultimate state of the entire structure, and therefore, the margin is implicitly considered during design.

Studies on parallelism have proposed an evaluation method based on the number of plastic hinges formed before the plastic collapse mechanism is reached[16)], and indices such as the strength redundancy index[17)] and sensitivity index[18)], which indicate the degree of reduction in the strength of a structure when a member is lost because of an unexpected event. Reference 10 used the method of Kanno and Ben-Haim[19)] to set the limit of the allowable degree of damage of the railway structure, after which it evaluated the number of members that can be lost without exceeding that limit.

2.2 Conceptualization of redundancy in this study

We used previous research as the basis for evaluating redundancy from the perspectives of both “margin” and “parallelism.” In this section, we discuss the concept of the limit state of a structure and summarize the concepts of margin and parallelism, after which we present a quantitative evaluation method for redundancy based on those concepts.

2.2.1 Conceptualization of the limit state

The limit state of a structure can be affected by the limits of elastic behavior and maximum strength. This paper aims to evaluate redundancy as an anti-catastrophe performance item, and therefore, we set the "state in which the entire structure collapses" as the limit state. The collapse state of the entire structure during an earthquake can be considered as collapse state A (Fig. 1(a)) in the horizontal direction, wherein the seismic action and restoring force are no longer balanced, and collapse state B (Fig. 1(b)) in the vertical direction, where the dead weight cannot be supported. For collapse state A, we used previous research[20] to define collapse as a state in which the horizonal seismic intensity becomes zero because of a decrease in the restoring force caused by the P-Δ effect. In addition, collapse state B is defined as a state in which the beam member fails under its dead weight because of a member that supports the vertical force no longer performing its function because of shear failure.

In this study, we defined it as the state in which the bending moment generated in the beam member under its own dead weight exceeds the maximum strength of the beam member. Collapse state B is assumed to occur when there is seismic action; however, we only considered collapse state B when there is no seismic action to avoid overcomplicating the evaluation method and consider applicability to design practice. Moreover, we consider a case in collapse state B, where the dead weight cannot be supported and where only the beam member loses its function; however, cases of earthquake damage to railway viaducts suggest that, in most cases, the vertical members are damaged first. Therefore, we decided to consider the failure of beam members because of the loss of the function of vertical members as the redundancy of railway viaducts that we consider in this paper.

2.2.2 Conceptualization of margin

We explain the concept of the margin based on the horizontal seismic intensity-horizontal displacement relationship of a typical railway bridge and viaduct (Fig. 2). The rebars of the reinforced concrete (RC) members yield at point Y as shown in the figure, and the structure becomes plastic. Then, the rebars of

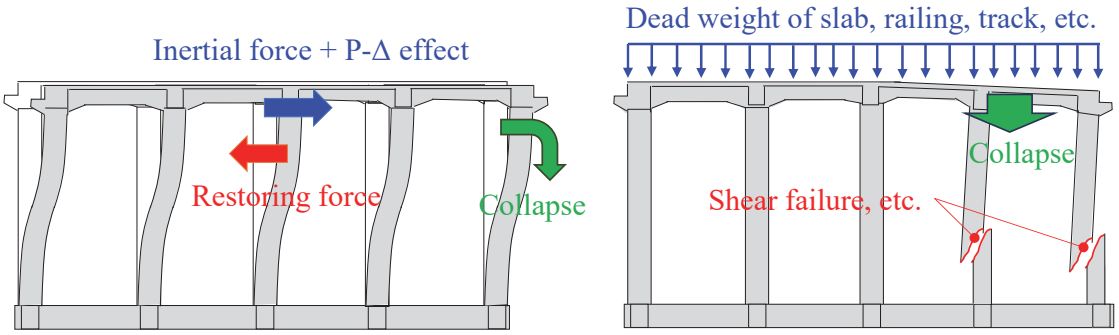

(a) Collapse state A (b) Collapse state B

Fig. 1 Definition of limit state when evaluating redundancy

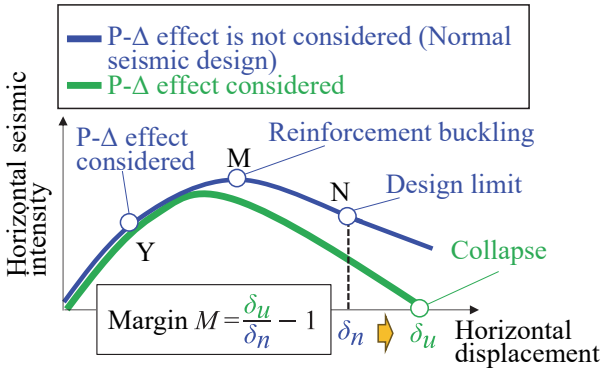

Fig. 2 Diagram of margin conceptualization

the RC members buckle at point M in the figure, and the strength decreases. In the current railway seismic design[1)], even under maximum displacement (point N in the figure), the rebars can support a load equivalent to point Y against the design earthquake motion. In contrast, when the P-Δ effect is considered, the horizonal seismic intensity-horizontal displacement relationship changes as indicated by the green line in Fig. 2. On this curve, the point where the horizontal seismic intensity becomes zero is the collapse state A.

Based on the idea where the anti-catastrophe concept is considered a set that cannot be covered by seismic design, the margin is evaluated from the perspective of how large the collapse displacement is relative to the design limit displacement (displacement at point N). Margin M is calculated using

$$M = \frac{\delta_u}{\delta_n} - 1 \tag{1}$$

where δ_u and δ_n represent the collapse displacement and design limit displacement, respectively. The aforementioned equation is constructed by considering the margin to be 0 when the design limit displacement (δ_n) is equal to the collapse displacement (δ_u). In addition, as described in Section 2.2.3, the margin is considered 0 when collapse state B occurs because of the disappearance of vertical members.

2.2.3 Conceptualization of parallelism

Parallelism is evaluated by the change in margin M for each of the lost members when member loss represents a condition where the member can no longer perform its function because of an unexpected event. Let n represent the total number of members, i represent the number of members to be lost, and j represent the number of combinations that do not result in collapse state B out of the possible combinations of lost members, ${}_nC_i$. Then, in the following equation, w_i represents the proportion of combinations that do not result in collapse state B when the number of lost members is i.

$$w_i = \frac{j}{{}_nC_i} \quad (i = 0, \ldots, n)(j = 0, \ldots, {}_nC_i) \tag{2}$$

This is defined as the weight for each number of lost members when evaluating redundancy. When i = 0 (the number of lost members is 0) and when j = 1 (there is no combination that will result in a collapse under its own dead weight), the weight $w_0 = 1$. In addition, when $i = n$ (all members are lost), the system does not function as a structural system, and therefore, j = 0, that is, $w_n = 0$.

2.3 Proposal of redundancy index S

The redundancy index (S) used to quantitatively evaluate redundancy is calculated by applying the following equation and Fig. 3:

$$S = \sum_{i=0}^{n-1} w_i M_i \tag{3}$$

where i, n, w_i, and M_i represent the number of lost vertical members, total number of vertical members, weight when the number of lost members is i, and mean margin value when collapse state B does not occur with the number of lost members i, respectively. This corresponds to the area when the vertical axis is the margin weighted by Eq. (2) and the horizontal axis is the number of lost members, as indicated in Fig. 3.

We explain why the margin is averaged for each assumed combination of lost positions when the number of lost members is i in Eq. (3). Further, we do not assume the cause of the loss of function of vertical members given the perspective of evaluating redundancy as an anti-catastrophe performance

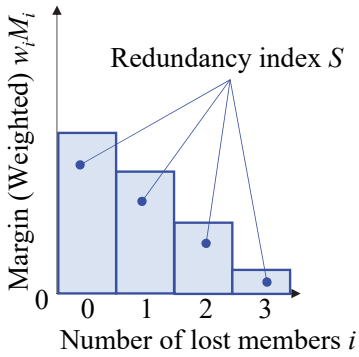

Fig. 3 Definition of redundancy index S

indicator. Therefore, we consider that member loss can occur equally in all locations. Each combination of lost positions when the number of lost members is i is an exclusive event that does not occur simultaneously, and therefore, it is believed that adding the margin for the combinations of lost positions can help overestimate the redundancy of a structure with a large number of vertical members. Therefore, we averaged the margin for loss combinations that do not result in collapse state B as a representative value of the margin for the number of lost members i. The horizontal seismic intensity-horizontal displacement relationship and deformation performance of the entire structure, which affects the margin, are roughly equivalent when excluding cases where the dead weight support state is extremely biased. Moreover, cases where the dead weight support state is extremely biased results in collapse state B, which will be considered a weight in Eq. (2). These two aspects indicate the validity of averaging the margin.

The above assumptions enable us to calculate the redundancy index S as follows :

[1] Calculate the design limit displacement using push-over analysis conducted in normal seismic design.
[2] Conduct a dead weight analysis by eliminating vertical members.
[3] If a collapse state B is not reached in [2], then a push-over analysis that considers the P-Δ effect is conducted to calculate the displacement at which the collapse state A would occur. The margin is calculated using Eq. (1).
[4] Steps [2]–[3] are repeated for each combination of the lost members to calculate w_i and M_i, and the redundancy index S is calculated using Eq. (3).

3. PROPOSED PRACTICAL QUANTITATIVE EVALUATION METHOD FOR REDUNDANCY

Redundancy can be quantitatively evaluated by calculating the redundancy index S; however, this calculation procedure requires a special analysis called push-over analysis that considers the P-Δ effect to be repeated many times for each combination of the lost members. It is considered difficult to apply it to practical design work. Therefore, we propose a method for calculating S within the scope of work performed in normal seismic design. We also describe a practical method to consider the P-Δ effect and lost member effect, after which we describe the procedure for quantitatively evaluating the redundancy index.

3.1 Practical method for considering the P-Δ effect

We assume that the entire structure can be evaluated using a single point-mass system model as shown in Fig. 4. We summarize the difference in the horizontal seismic intensity-horizontal displacement relationship depending on whether the P-Δ effect is considered. A typical railway bridge or viaduct can

be represented as a single point-mass system model, and therefore, the above assumption is somewhat versatile.

Figure 5 presents a diagram of the practical method to consider the P-Δ effect. In normal seismic design, a push over analysis is conducted that ignores the P-Δ effect, and thus, the blue line a) in Fig. 5 is calculated during the normal design process. Meanwhile, in a single point-mass system model with a structural height of h, the reduction in the restoring force attributed to the P-Δ effect is theoretically shown as a straight line with a slope of $-1/h$ when shown in the horizontal displacement-horizontal seismic intensity relationship (orange line b) in Fig. 5). Therefore, adding the blue line a) and orange line b) enables performing an evaluation that considers the P-Δ effect (green line in Fig. 5).

3.2 Practical method for considering the lost member effect

We consider the change in the horizontal seismic intensity-horizontal displacement relationship in a structure with n vertical members when i vertical members are lost. Assuming that the horizontal stiffness decreases with a decrease in the number of lost vertical members, the reduction factor α is evaluated using

$$\alpha = 1 - \frac{i}{n} \tag{4}$$

Figure 6 displays a diagram of a practical method for considering the effect of lost members. Multiplying the push over analysis results (blue line i) in Fig. 6) under conditions where all members are present by the reduction factor α of horizontal stiffness calculated using Eq. (4) enables evaluating the effect of the lost members (light blue line ii) in Fig. 6). The above equation is valid under ideal conditions where all vertical members have the same cross section and reinforcement arrangement, and the effects of the axial force fluctuations are ignored. Therefore, in Section 4.3, we confirm the validity

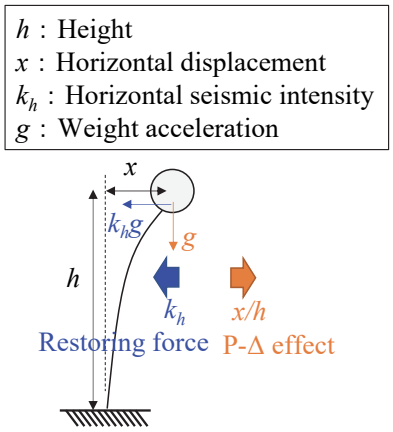

Fig. 4 Overview of one point-mass system model

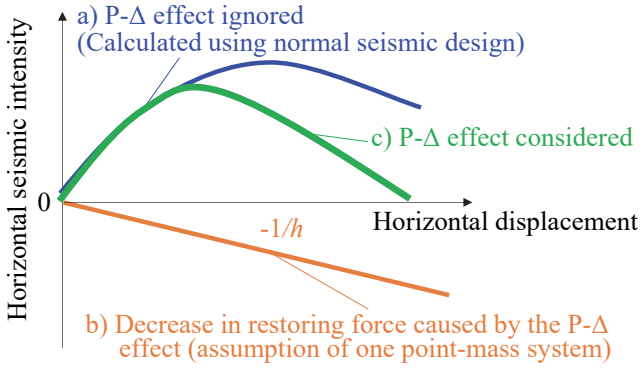

Fig. 5 Practical method of considering the P-Δ effect

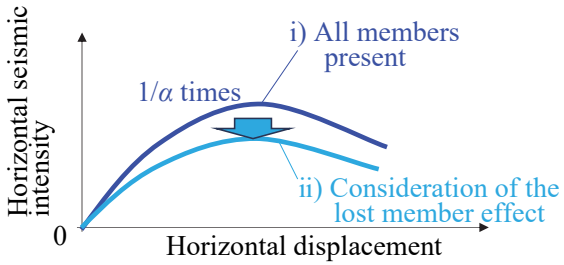

Fig. 6 Practical method of considering the lost member effect

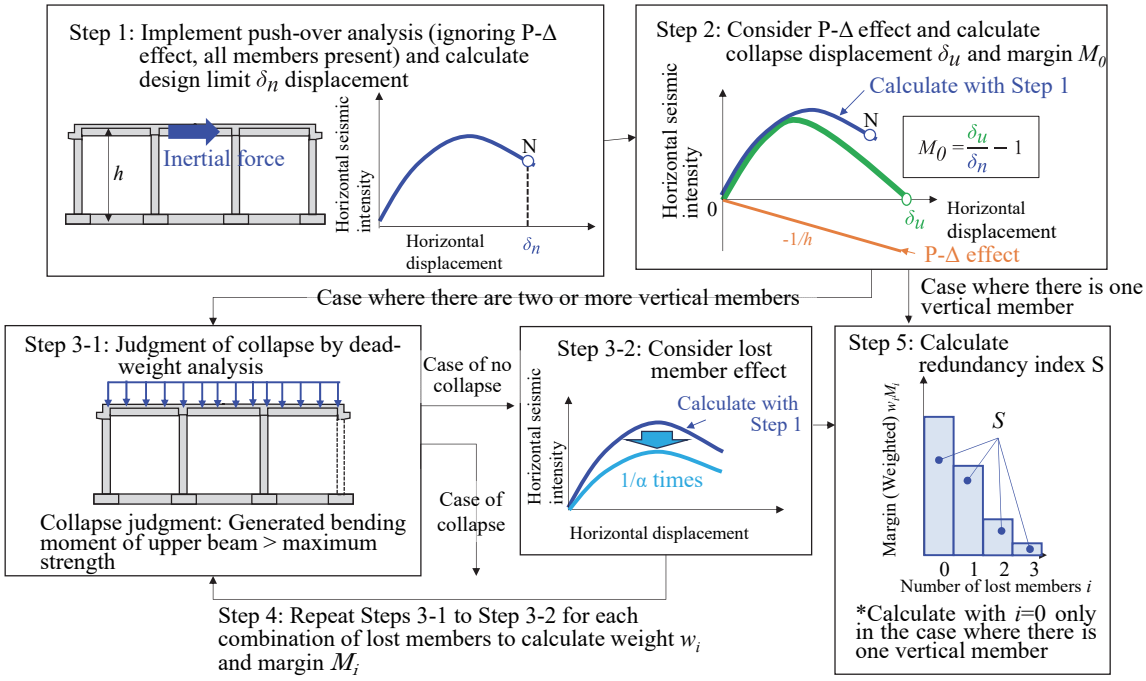

Fig. 7 Flowchart of the practical quantitative evaluation method for redundancy

of Eq. (4) from the perspective of practically evaluating redundancy using a specific railway viaduct.

3.3 Procedure for the practical quantitative evaluation of redundancy

Based on the above context, the procedure for the practical quantitative evaluation of redundancy is shown in Fig. 7 and presented below:

- Step 1: Perform the push-over analysis (ignoring P-Δ effect, all members present) and calculate the design limit displacement, δ_n.
- Step 2: Calculate collapse displacement δ_u and margin M_0 by considering the P-Δ effect using the method described in Section 3.1.
- Step 3-1: Perform the dead weight analysis and determine the occurrence of collapse (whether bending moment of the upper beam is greater than the maximum strength).
- Step 3-2: If no collapse is determined in Step 3-1, consider the lost member effect using the method described in Section 3.2.
- Step 4: Repeat Steps 3-1 and 3-2 for each combination of the lost members and calculate the weight w_i and margin M_i.
- Step 5: Calculate the redundancy index (S) using Eq. (3).

Among these steps, Step 1 is conducted in normal seismic design, and Steps 2–5 include relatively simple analyses and calculations. Therefore, using this method enables the evaluation of redundancy with roughly the same amount of work as in conventional design.

4. VALIDATION OF THE PRACTICAL METHOD FOR CONSIDERING THE P-Δ AND LOST MEMBER EFFECTS

4.1 Overview

We conduct a detailed push-over analysis on a rigid frame viaduct, which directly considers the P-Δ effect and member loss in the analysis. Further, we validate the results by comparing them with the

results of the practical method of considering the P-Δ effect and lost member effect described in the previous section.

The structure analyzed for verifying the validity is a three-span rigid frame viaduct of a direct foundation type (Fig. 8) modeled using a three-dimensional frame model in accordance with the Seismic Standards[1]. The P-Δ effect is considered a geometric stiffness. However, the ground spring is assumed to be linear because of the limitations of the calculation tool, and the stiffness of the member after point M is assumed to be a small positive value. In addition, this section confirms the validity of the practical method for considering the P-Δ effect and lost member effect, and therefore, the upper beams are assumed to be linear members so that they do not collapse under their own dead weight. However, depending on the location and number of lost members, there are cases where the cross-sectional strength distribution of the upper beams exceeds the cross-sectional strength (about 4,000 kN·m) under a dead weight state, which results in collapse state B (Fig. 1(b)).

4.2 Validation of the practical method for considering the P-Δ effect

Figure 9 shows the horizontal seismic intensity-horizontal displacement relationship at the top of the viaduct caused by the push-over analysis in the bridge-axis direction. The N point, which is the design limit displacement, is plotted as a square to represent the deformation performance. The figure indicates that the horizontal seismic intensity decreased because of the P-Δ effect after the point where the horizontal seismic intensity-horizontal displacement relationship bends considerably. Further, no significant difference in deformation performance can be observed regardless of the P-Δ effect.

Figure 10 depicts the horizontal seismic intensity-horizontal displacement relationship calculated using the proposed method. The structural height *h* of the rigid-frame viaduct is calculated as the length from the top of the underground beam, which undergoes bending deformation, to the top of the column.

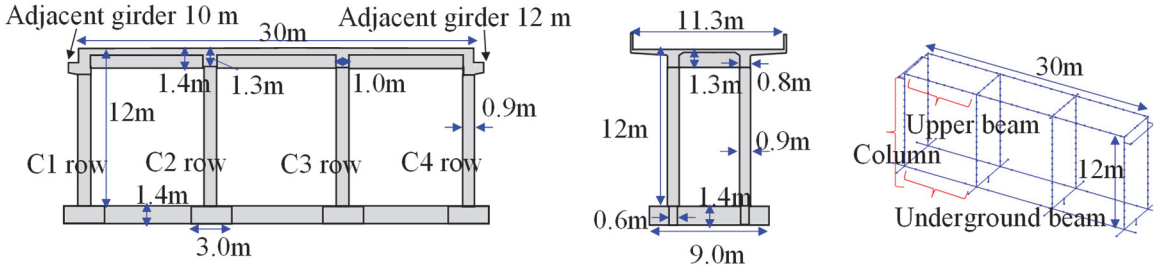

(a) Side view (b) Cross-section (c) 3D frame model

Fig. 8 Target structure

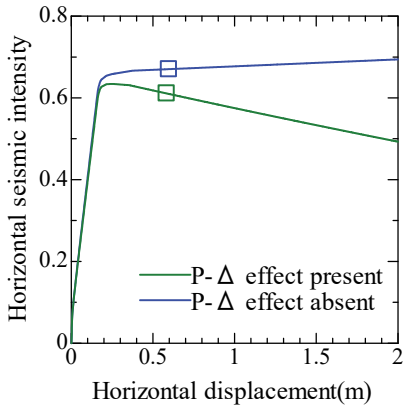

Fig. 9 Push-over analysis results with and without the P-Δ effect

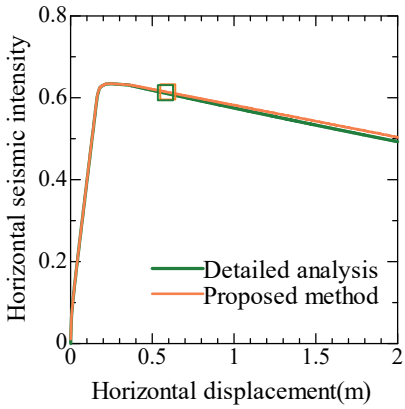

Fig. 10 Validation results of practical method of considering the P-Δ effect

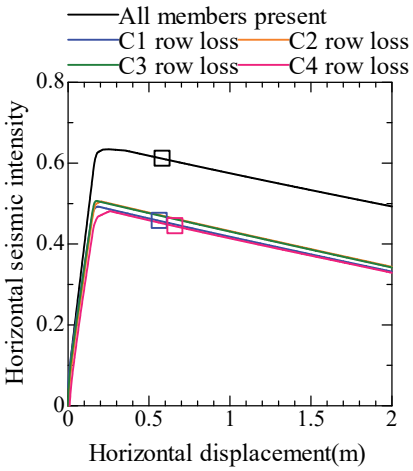

Fig. 11 Horizontal seismic intensity-horizontal displacement relationship when one column member row is lost

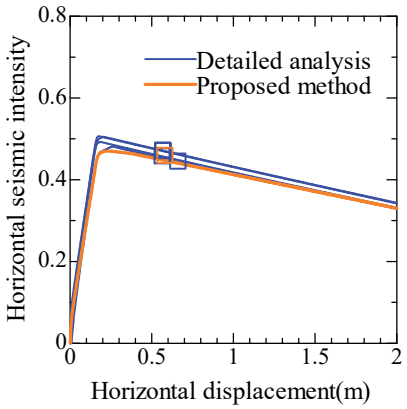

Fig. 12 Confirmation results of the practical method for considering the lost member effect (1 row loss)

This figure shows that the proposed method can effectively express the results of the detailed analysis. The validity of the practical method for considering the P-Δ effect was confirmed.

4.3 Validation of the practical method for considering the lost member effect

A push-over analysis was conducted for the analysis model considering the combination of lost vertical members for each column row in the bridge-axis direction considering the P-Δ effect. Figure 11 shows the horizontal seismic intensity-horizontal displacement relationship and deformation performance (design limit displacement) when one column row is lost. The figure confirms the results when all members are present. As indicated in the figure, the horizontal seismic intensity-horizontal displacement relationship is the same for all lost positions. Further, we can see that the deformation performance is the same as that when all members are present. Figure 12 presents a comparison of the horizontal seismic intensity-horizontal displacement relationship and deformation performance (design limit displacement) between the proposed method and detailed analysis when one column row is lost. This figure indicates that the horizontal seismic intensity at the same displacement is slightly smaller in the proposed method than that in the detailed analysis. This is believed to be caused by the increase in the cross-sectional strength of the column members because of the effect of axial force fluctuation. Although the proposed method does not completely match the results of the detailed analysis, it can generally express the results. Figure 13 shows the bending moment distribution under the dead-weight state in each case. The cases of C1 row loss and C4 row loss, where the end row is lost, exhibit a negative bending of about 10,000 kN・m caused by the effect of the structural system bearing the weight of the adjacent girder in the form of a cantilever beam, which exceeds the cross-sectional strength of the upper beam (about 4,000 kN・m) and results in collapse state B. Figure 7 shows that the horizontal seismic intensity-horizontal displacement relationship does not need to be evaluated in such cases; however, even if the proposed method is used, the results of the detailed analysis can be adequately expressed as described above.

Figure 14 shows the horizontal seismic intensity-horizontal displacement relationship and deformation performance (design limit displacement) when two column rows are lost. Figure 15 presents a comparison of the horizontal seismic intensity-horizontal displacement relationship and deformation performance (design limit displacement) of the proposed method and the detailed analysis. These figures indicate that, with the exception of the cases of C1C2 row loss and C3C4 row loss, the horizontal seismic intensity-horizontal displacement relationship is equivalent, and the deformation performance is the same as that when all members are present. Although the horizontal seismic intensity at the same displacement is slightly smaller in the proposed method than that in the detailed analysis because of the effect of axial force fluctuations, the detailed analysis can be generally expressed overall.

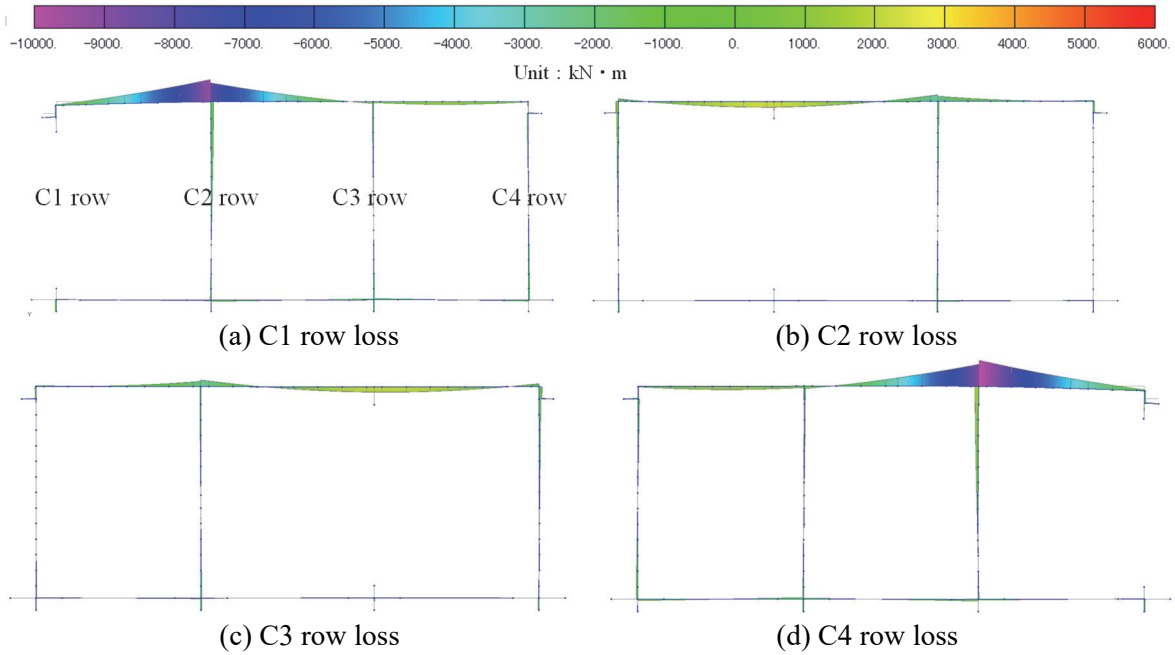

(a) C1 row loss (b) C2 row loss

(c) C3 row loss (d) C4 row loss

Fig. 13 Bending moment distribution under dead-weight state (1 row of lost members, deformation magnification factor of 5)

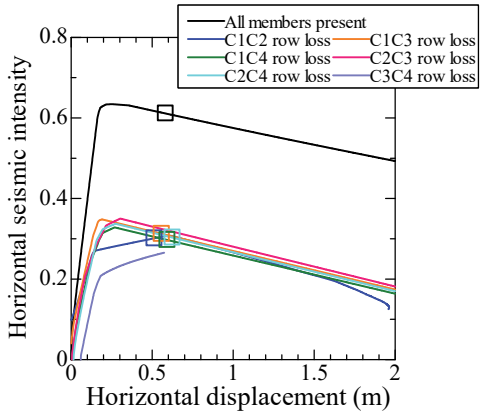

Fig. 14 Horizontal seismic intensity-horizontal displacement relationship when two column member rows are lost

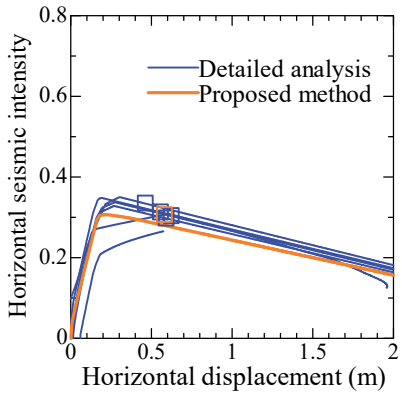

Fig. 15 Confirmation results of the practical method considering the lost member effect (2 row loss)

The cases of C1C2 row loss and C3C4 row loss exhibited an unstable push-over analysis because of the detailed analysis partway through the analysis.

We discuss the above results after considering the examples of bending moment distribution and axial force distribution in the dead-wight state (Figs. 16 and 17). These figures confirm that, in both cases, the bending moment generated at the end of the upper beam exceeds the cross-sectional strength of the upper beam (about 4,000 kN・m), which results in collapse state B. The cases of C1C2 row loss and C3C4 row loss exhibit a negative bending of up to about 30,000 kN・m in the upper beam, which is a compressive axial force of about 6,000 kN in the column next to the lost member and the tensile axial force of about 2,000 kN in the adjacent column. This is an extreme case in which the bending moment and axial force are several times larger than those in other loss combinations. A tensile axial force occurs under a dead-weight state, and therefore, cases with extreme cross-sectional force distribution exhibit considerable deviation in the horizonal seismic intensity-horizontal displacement relationship from the

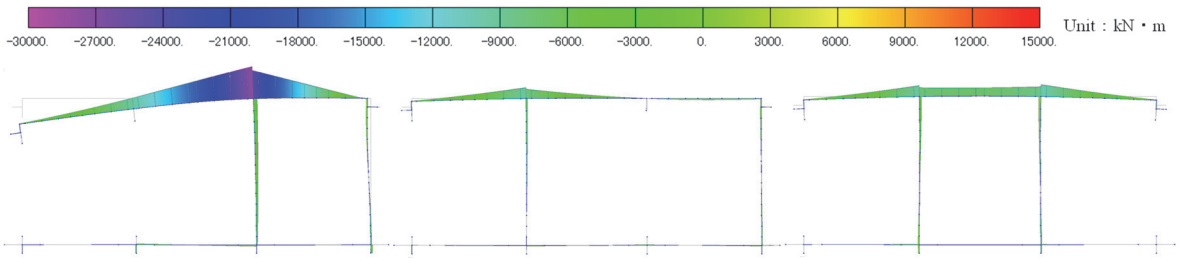

(a) C1C2 row loss (b) C1C3 row loss (c) C1C4 row loss

(d) C2C3 row loss (e) C2C4 row loss (f) C3C4 row loss

Fig. 16 Bending moment distribution under dead-weight state (2 rows of lost members, deformation magnification factor of 5)

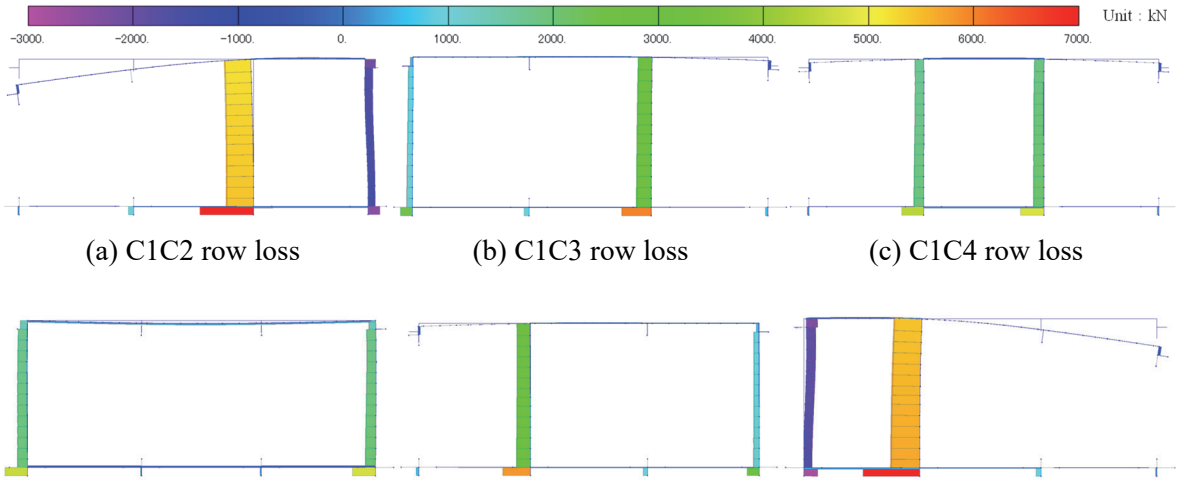

(a) C1C2 row loss (b) C1C3 row loss (c) C1C4 row loss

(d) C2C3 row loss (e) C2C4 row loss (f) C3C4 row loss

Fig. 17 Axial force distribution under dead-weight state (2 rows of lost members, deformation magnification factor of 5)

proposed method because of the push over analysis not being able to be conducted in a stable manner. However, there is no need to evaluate the horizontal seismic intensity-horizontal displacement relationship because this results in collapse state B, and it does not affect our results in terms of the practical evaluation of redundancy. Meanwhile, as described in Fig. 7, cases such as C2C3 row loss or C1C3 row loss are those where the cross-sectional force distribution is large in a dead-weight state where the horizontal seismic intensity-horizontal displacement relationship does not need to be evaluated. However, as shown in Figs. 14 and 15, the results of the detailed analysis can be sufficiently expressed even if the horizontal seismic intensity-horizontal displacement relationship and deformation performance are calculated using the proposed method. In other words, we validated the practical method of considering the lost member effect within a range that includes conditions with a considerably severe dead-weight state.

5. QUANTITATIVE EVALUATION OF REDUNDANCY USING THE PROPOSED METHOD

5.1 Calculation overview

The evaluation in Section 4 confirmed the validity of the practical method for considering the P-Δ effect and lost member effect in the redundancy evaluation method proposed in Section 3. In this section, we use the proposed method to estimate the redundancy for a rigid-frame viaduct that meets the current Seismic Standards[1]. We model the negative slope of the members after point M and the nonlinearity of the ground spring using a two-dimensional frame model, as is done with normal seismic design.

Table 1 lists the cases to be calculated. Cases 1–5 are cases where the number of spans is different, with the same conditions of reinforcement and cross-sectional dimensions. Case 6 is based on Case 5; however, only the cross-sectional dimensions and reinforcement of the upper beams are changed. Figure 18 shows the side view and cross-sectional view of Case 5 as an example of the target viaduct. This is a rigid-frame viaduct that meets the Seismic Standards[1] shown in the reference[21]. In addition, the reinforcement diagram of the columns common to Cases 1–6 is presented in Fig. 19, the reinforcement diagram of the upper beams (Type 1) of Cases 1–5 is shown in Fig. 20(a), and the reinforcement diagram of the upper beams (Type 2) of Case 6 is depicted in Fig. 20(b). Compared to Type 1, Type 2 has a larger cross-sectional dimension and amount of reinforcing bars, which improves the cross-sectional strength and cross-sectional rigidity. Further, the ground condition of each case is the same as that shown in Fig. 21, which is a condition classified as G3 ground (ordinary ground) in the Seismic Standards[1]. For each case, we calculate the vibration characteristics and deformation performance using the normal seismic design to calculate redundancy.

5.2 Calculation of vibration characteristics and deformation performance and the confirmation of performance with respect to the L2 earthquake motion

For each case, we conducted a push-over analysis without considering the P-Δ effect, with the vibration characteristics calculated as described in the Seismic Standards[1]: An equivalent natural period T_{eq}, seismic coefficient at the turning point of the entire structure k_{heq} (henceforth, "yielding seismic

Table 1 List of cases to be calculated

Case	1	2	3	4	5	6
Number of spans	1	2	3	4	5	5
Cross-section of upper beam	Type1					Type2

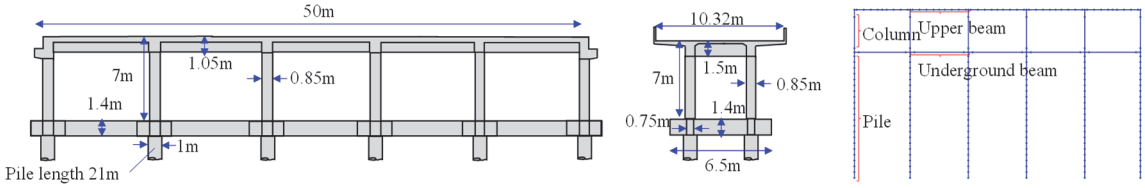

(a) Side view (b) Cross section (c) 2D frame model

Fig. 18 Example of rigid-frame viaduct to be examined (Case 5)

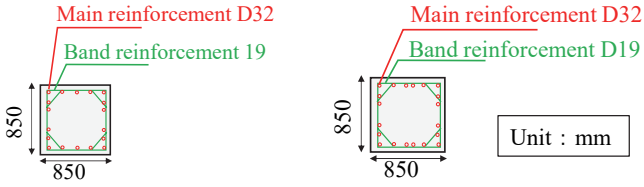

(a) Middle column (b) End column

Fig. 19 Column reinforcement diagram

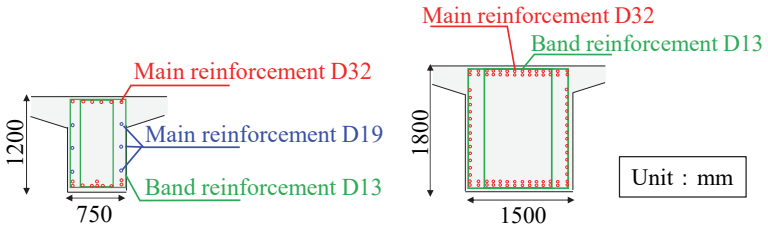

(a) Type 1 (b) Type 2

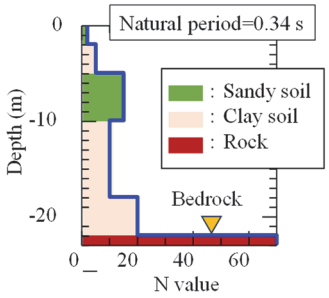

Fig. 21 Ground condition

Fig. 20 Upper beam reinforcement diagram

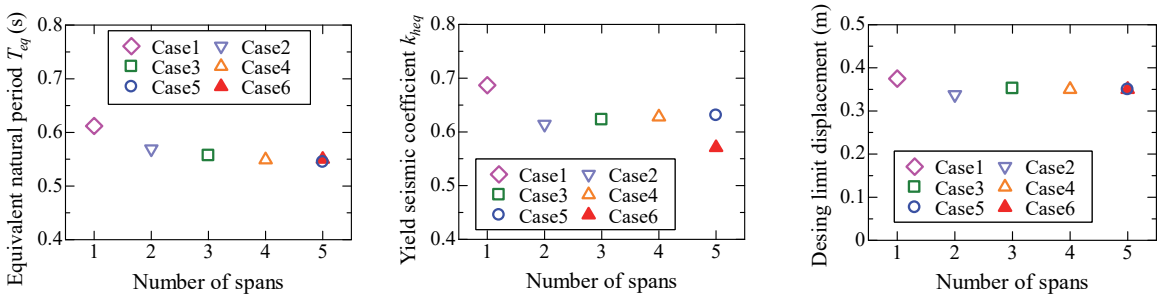

(a) Equivalent natural period (b) Yield seismic coefficient (c) Design limit displacement

Fig. 22 Vibration characteristics and deformation performance summary results

coefficient" for convenience) of the entire structure, and deformation performance (design limit displacement: N-point displacement). Figure 22 depicts the vibration characteristics and deformation performance for each number of spans. This figure indicates that cases where the number of spans is 2–5 results in a roughly equivalent number of spans, vibration characteristics, and deformation performance. This is attributed to the fact that the reduction in the horizontal stiffness of the columns and weight of the superstructure caused by the different number of spans is roughly equivalent. Meanwhile, cases where the number of spans is 1 exhibit slightly different vibration characteristics and deformation performance. This can be attributed to the influence of the end points (e.g., strength of the end columns and weight of adjacent girders) becoming relatively larger with a smaller number of spans. In addition, Case 6 has large cross-sectional dimensions of the upper beams (Fig. 20(b)), and the yielding seismic coefficient becomes somewhat smaller because of the larger inertial force.

We calculate the maximum response displacement δ_{max} for the standard L2 earthquake motion (spectrum II)[1)] on G3 ground using the nonlinear response spectrum[1)]. Then, we consider the ratio to the design limit displacement δ_N (δ_{max}/δ_N) as the verification value for the L2 earthquake motion and organize the verification values by the number of spans (Fig. 23). This resulted in the verification values for the L2 earthquake motion being approximately equivalent at about 0.6–0.7. In other words, each case can be said to be a structure evaluated to have similar performance under the current seismic design.

5.3 Calculation of the redundancy index

The redundancy index S for each case is calculated based on the procedure described in Section 3.3. In Step 1, a normal push-over analysis that does not consider the P-Δ effect is conducted, which uses the results calculated in Section 5.2. In Step 2, the horizontal seismic intensity-horizontal displacement relationship that considers the P-Δ effect is calculated. Figure 24 shows an example of Case 5. The figure indicates the horizontal seismic intensity-horizontal displacement relationship calculated in Step 1 without considering the P-Δ effect. This figure suggests that the horizontal displacement leading to the collapse in Case 5 (horizontal displacement at which horizontal seismic intensity becomes zero) is about

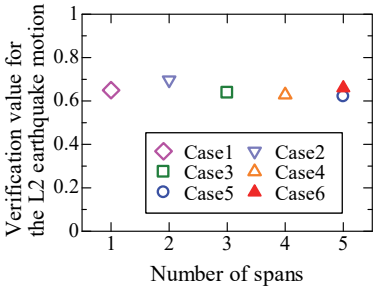

Fig. 23 Relationship between the number of spans and verification value for the L2 earthquake motion

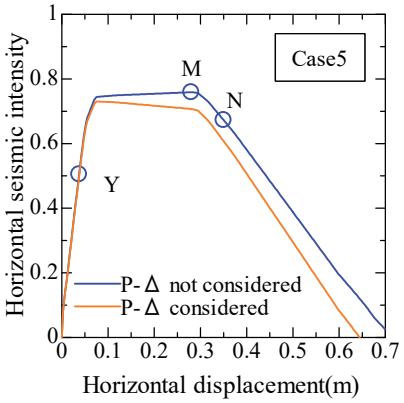

Fig. 24 Example of the horizontal seismic intensity-horizontal displacement relationship considering the P-Δ effect

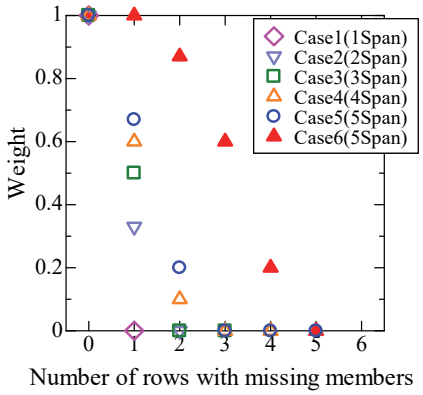

Fig. 25 Results of weight calculation using dead-weight analysis

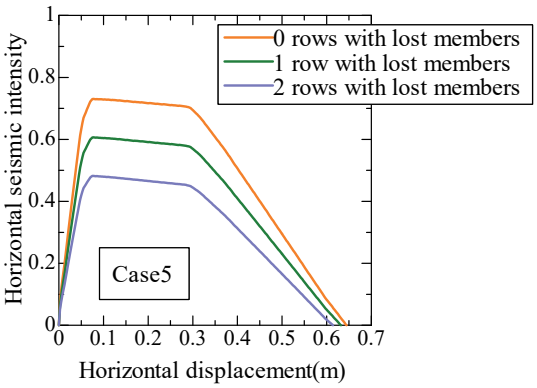

Fig. 26 Example of the horizontal seismic intensity-horizontal displacement relationship considering the lost member effect

0.65 m.

In Step 3-1 to Step 4, a dead-weight analysis is conducted for each combination of the lost vertical members of the rigid-frame viaduct. The combinations in which the bending moment of the upper beams is below the maximum strength are identified, with the weight (proportion of structures that do not collapse under their own dead weight) calculated based on Eq. (2) (Fig. 25). This figure indicates that a larger number of spans increase the number of combinations that do not collapse under their own dead weight even with a lost member and increase the weight for each lost member row. In addition, Case 6, which has a large cross-sectional strength of the upper beams, has a large weight because it is less likely to collapse under its own dead weight when a member is lost compared to the other cases. In Step 3-2 to Step 4, the skeleton curve for the combinations judged not to collapse under their own weight is calculated. The skeleton curve that does not consider the P-Δ effect is corrected by the P-Δ effect after considering the effect of the lost members (Fig. 26). This figure indicates that an increasing number of rows with lost members resulted in a smaller skeleton curve and a smaller collapse displacement at which the horizonal seismic intensity becomes zero.

In Step 5, the margin (weighted) is calculated for each number of rows with lost members for each structure using Eqs. (1) and (2), and then, the redundancy index (S) is calculated using Eq. (3) (Fig. 27). This figure shows that an increasing number of spans increases the redundancy index S because of the added effect of parallelism. In addition, in Case 6, where the cross-sectional strength of the upper beams

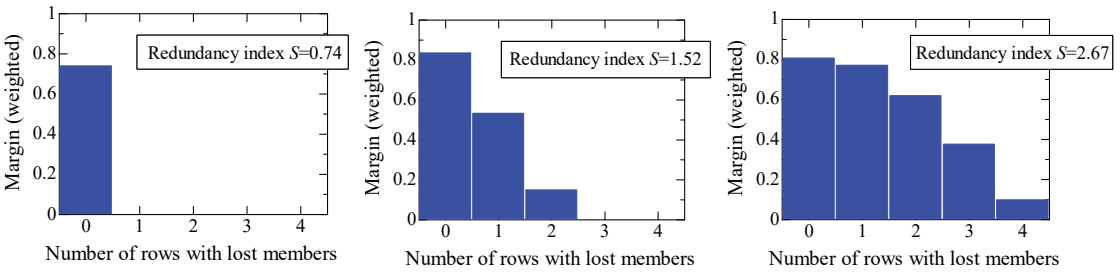

(a) Case 1 (1 span, upper beam Type 1) (b) Case 5 (5 spans, upper beam Type 1) (c) Case 6 (5 spans, upper beam Type 2)

Fig. 27 Example of the calculation results of redundancy index *S*

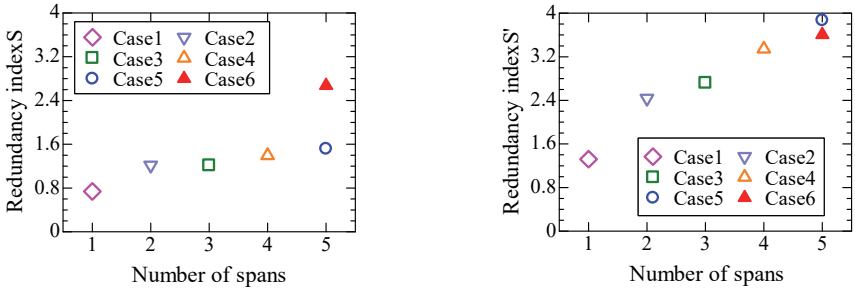

(a) Result using proposed method (collapse caused by dead weight considered) (b) Result ignoring collapse caused by dead weight

Fig. 28 Relationship between the number of spans and redundancy index *S*

is large, the effect of parallelism is greater, and the redundancy index *S* is larger. This indicates that the proposed method can be used for evaluating redundancy by considering the collapse displacement (margin) relative to the design limit displacement and the number of members (parallelism).

5.4 Discussion on the redundancy index (S)

Figure 28(a) displays the relationship between *S* calculated in Section 5.3 and the number of spans. For the following discussion, we show *S*' calculated under the condition that all weights in Eq. (2) are 1, i.e., ignoring the collapse under a dead-weight state (Fig. 1(b)) in Fig. 28(b). In each case, the redundancy index tended to increase with an increasing number of spans; however, the amount of increase in Fig. 28(b) was greater. In addition, the redundancy indices of Cases 5 and 6, which have different cross-sectional strengths of the upper beams, are clearly different in Fig. 28(a); however, they are similar in Fig. 28(b). Thus, considering the collapse under a dead-weight state enables the prevention of an overestimation of redundancy caused by the large number of vertical members and the expression of the tendency that differs in the cross-sectional strength of the upper beams that affect redundancy.

Although each case was evaluated as having the same performance in the current seismic design, we confirmed clear differences in redundancy based on the number of spans (number of members) and cross-sectional strength of the upper beams.

6. CONCLUSION

In this study, we focused on redundancy, which is one of the anti-catastrophe performance items, and we proposed a quantitative evaluation method for the same. The specific proposals made in this study and the findings are summarized below:

- We proposed an index to quantitatively evaluate the redundancy of a structure from the following two perspectives, considering the state where the entire structure collapses as the limit state:

"margin", which is the displacement that leads to a collapse because of the P-Δ effect with respect to the design limit displacement, and "parallelism", which is the change in the margin when a vertical member is lost.

- We used a push-over analysis conducted in a normal seismic design as the basis to propose a practical method for evaluating the margin and parallelism by considering the P-Δ effect and member loss, and we validated the method by comparing its results with a detailed analysis.
- We used a general railway rigid-frame viaduct as an example for calculating the redundancy using the proposed method, where we confirmed that the redundancy of each structure can be quantitatively evaluated. Further, we quantitatively showed that a larger number of spans and a greater cross-sectional strength of the upper beams increased redundancy.

In future, we plan to calculate redundancy for other structural types and structures with different performance against the L2 earthquake motion, and we organize the direction of the seismic performance of railway bridges and viaducts.

REFERENCES

1) Railway Technical Research Institute: *Design Standards for Railway Structures and Commentary (Seismic Design)*, Maruzen Co., Ltd, Tokyo, 2012 (in Japanese).
2) Toma, J.: Ideal Earthquake and Tsunami Resistance for Nuclear Power Plants, *Journal of Nuclear Science and Technology*, Vol. 55, No. 8, pp. 23–27, 2013 (in Japanese).
3) Honda, R., Akiyama, M., Kataoka, S., Takahashi, Y., Nozu, A. and Murono, Y.: Seismic Design Method to Consider "Anti-Catastrophe" Concept a Study for the Draft Design Codes, *Journal of Japan Society of Civil Engineers*, *Series A1 (Structural Engineering & Earthquake Engineering)*, Vol. 72, No. 4, (*Journal of Earthquake Engineering*, Vol. 35), pp. I_459–I_472, 2016 (in Japanese).
4) Nozu, A., Murono, Y., Motoyama, H. and Honda, R.: "Anti-Catastrophe" Concept in Design Standards for Railway and Port Structures, *Journal of Japan Society of Civil Engineers*, *Series A1 (Structural Engineering & Earthquake Engineering)*, Vol. 72, No. 4, (*Journal of Earthquake Engineering*, Vol. 35), pp. I_448–I_458, 2016 (in Japanese).
5) Takahashi, Y., Akiyama, M., Kataoka, S. and Honda, R.: Analysis of "Anti-Catastrophe" Property in JRA and Foreign Design Specifications for Highway Bridges, *Journal of Japan Society of Civil Engineers*, *Series A1 (Structural Engineering & Earthquake Engineering)*, Vol. 72, No. 4, (*Journal of Earthquake Engineering*, Vol. 35), pp. I_821–I_830, 2016 (in Japanese).
6) Honda, R.: Study for Implementation of Anti-Catastrophe-Oriented Seismic Design, *Journal of Japan Society of Civil Engineers*, *Series A1 (Structural Engineering & Earthquake Engineering)*, Vol. 72, No. 4, (*Journal of Earthquake Engineering*, Vol. 37), pp. I_1078–I_1086, 2018 (in Japanese).
7) Takeda, A. and Nishimura, T.: A Study for Introducing the Concept "Anti- Catastrophe" to Seismic Deign of Bridge, *Journal of Japan Society of Civil Engineers*, *Series A1 (Structural Engineering & Earthquake Engineering)*, Vol. 75, No. 4, (*Journal of Earthquake Engineering*, Vol. 38), pp. I_688–I_700, 2019 (in Japanese).
8) Nishimura, T., Murono, Y., Toyooka, A. and Igarashi, A.: Dead Weight Compensation Mechanism for Improving Anti-Catastrophic Performance of Viaducts: Feasibility Investigation, *Journal of Japan Society of Civil Engineers*, *Series A1 (Structural Engineering & Earthquake Engineering)*, Vol. 75, No. 4, (*Journal of Earthquake Engineering*, Vol. 38), pp. I_569–I_578, 2019 (in Japanese).
9) Toyooka, A., Murono, Y. and Saito, M.: Development of the Collapse Direction Control Device for Improving Anti-Catastrophe Performance of a Viaduct, *RTRI Report*, Vol. 32, No. 9, pp. 47–52, 2018 (in Japanese).
10) Murono, Y., Tanaka, K., Saito, M., Sakai, K. and Toyooka, A.: Proposal of Evaluation Method for Anti-Catastrophe Performance of Railway Structures in Seismic Design, *Journal of Japan Society of Civil Engineers*, *Series A1*, Vol. 75, No. 3, pp. 336–349, 2019 (in Japanese).
11) Negishi, Y. and Otake, K.: Design Procedure Proposals and Seismic Design Examples for Crisis

Resilience, *Association of Water and Sewage Works Consultants Japan Technical Report Collection*, Vol 37, pp. 19–24, 2023 (in Japanese).
12) Nomura, K., Uemura, K. and Takahashi, Y.: Anti-Catastrophe Performance Oriented Structural Planning of Continuous Truss Bridges Based on Mechanical Skeleton, *Journal of Japan Society of Civil Engineers*, *Series A1 (Structural Engineering & Earthquake Engineering)*, Vol. 7, No. 4, (*Journal of Earthquake Engineering*, Vol. 41), pp. I_565–I_579, 2022 (in Japanese).
13) Architectural Institute of Japan: *Redundancy and Robustness in Building Structural Design*, Maruzen Co., Ltd, Tokyo, 2012 (in Japanese).
14) Tadokoro, T., Tanaka, K., Tanimura, Y., Kurokawa, H., Hattori, H. and Murono, Y.: Evaluation Method of Limit State of Collapse for Reinforced Concrete Columns, *Journal of Japan Society of Civil Engineers*, *Series E*, Vol. 64, No. 2, pp. 298–313, 2008 (in Japanese).
15) Nakamura, H.: Elastic-Plastic Dynamic Buckling Analysis of a Steel Circular Pier, *Journal of Japan Society of Civil Engineers*, No. 549, I-37, pp. 205–219, 1996 (in Japanese).
16) Bertero, R. D. and Bertero, V. V.: Redundancy in Earthquake-Resistant Design, *Journal of Structural Engineering*, Vol. 125, No. 1, pp. 81–88, 1999.
17) Frangopol, D. M. and Curley, J. P.: Effects of Damage and Redundancy on Structural Reliability, *Journal of Structural Engineering,* Vol. 113, No. 7, pp. 1533–1549, 1987.
18) Ito, T., Ohi, K. and Li, Z.: A Sensitivity Analysis Related to Redundancy of Framed Structures Subjected to Vertical Loads, *Journal of Structural and Construction Engineering* (*Transactions of AIJ*), Vol. 593, pp. 145–151, 2005 (in Japanese).
19) Kanno, Y. and Ben-Haim, Y.: Redundancy and Robustness, or When is Redundancy Redundant ?, *Journal of Structural Engineering,* Vol. 137, pp. 935–945, 2011.
20) Goto, Y., Ebisawa, T. and Bach, N. V.: Three-Dimensional Dynamic Collapse of Thin-Walled Steel Piers under Seismic Accelerations, *Journal of Japan Society of Civil Engineers, Series A1 (Structural Engineering & Earthquake Engineering)*, Vol. 73, No. 3, pp. 512–531, 2017 (in Japanese).
21) Railway Technical Research Institute: *Verification Example of RC Rigid Frame Viaducts by Design Standards for Railway Structures and Commentary (Seismic Design),* Railway Research-Culture Promotion Foundation, 2005 (in Japanese).

(Original Japanese Paper Published: January 2025)
(English Version Submitted: April 07, 2025)
(English Version Accepted: April 26, 2025)